



## New high-spin states of $^{142}_{58}\text{Ce}$ and $^{140}_{56}\text{Ba}$ from fusion-fission reactions: Proton excitations in the $N = 84$ isotones

T. Venkova, M.-G. Porquet, I. Deloncle, P. Petkov, A. Astier, A. Prevost, F. Azaiez, A. Bogachev, A. Buta, D. Curien, et al.

### ► To cite this version:

T. Venkova, M.-G. Porquet, I. Deloncle, P. Petkov, A. Astier, et al.. New high-spin states of  $^{142}_{58}\text{Ce}$  and  $^{140}_{56}\text{Ba}$  from fusion-fission reactions: Proton excitations in the  $N = 84$  isotones. *European Physical Journal A*, 2007, 34, pp.349-353. 10.1140/epja/i2007-10526-y . in2p3-00244925

**HAL Id: in2p3-00244925**

**<https://hal.in2p3.fr/in2p3-00244925>**

Submitted on 7 Feb 2008

**HAL** is a multi-disciplinary open access archive for the deposit and dissemination of scientific research documents, whether they are published or not. The documents may come from teaching and research institutions in France or abroad, or from public or private research centers.

L'archive ouverte pluridisciplinaire **HAL**, est destinée au dépôt et à la diffusion de documents scientifiques de niveau recherche, publiés ou non, émanant des établissements d'enseignement et de recherche français ou étrangers, des laboratoires publics ou privés.

# New high-spin states of $^{142}_{58}\text{Ce}$ and $^{140}_{56}\text{Ba}$ from fusion-fission reactions: Proton excitations in the $N = 84$ isotones

Ts. Venkova<sup>1,2</sup>, M.-G. Porquet<sup>1</sup>, I. Deloncle<sup>1</sup>, P. Petkov<sup>1,2</sup>, A. Astier<sup>1</sup>, A. Prévost<sup>1</sup>, F. Azaiez<sup>3a</sup>, A. Bogachev<sup>4</sup>, A. Buta<sup>3</sup>, D. Curien<sup>3</sup>, O. Dorvaux<sup>3</sup>, G. Duchêne<sup>3</sup>, J. Durell<sup>5</sup>, B.J.P. Gall<sup>3</sup>, M. Houry<sup>6b</sup>, F. Khalfallah<sup>3</sup>, R. Lucas<sup>6</sup>, M. Meyer<sup>7</sup>, I. Piqueras<sup>3</sup>, N. Redon<sup>7</sup>, A. Roach<sup>5</sup>, M. Rousseau<sup>3</sup>, O. Stézowski<sup>7</sup>, and Ch. Theisen<sup>6</sup>

<sup>1</sup> CSNSM, IN2P3-CNRS/Université Paris-Sud, 91405 Orsay, France

<sup>2</sup> Institute of Nuclear Research and Nuclear Energy, Bulgarian Academy of Sciences, 1784 Sofia, Bulgaria

<sup>3</sup> IPHC-DRS, Université Louis Pasteur/IN2P3-CNRS, 67037 Strasbourg Cedex 2, France

<sup>4</sup> JINR, Joliot-Curie 6, 141980, Dubna, Moscow region, Russia

<sup>5</sup> Dept. of Physics and Astronomy, University of Manchester, M13 9PL, United Kingdom

<sup>6</sup> Commissariat à l'Énergie Atomique, CEA/DSM/DAPNIA/SPhN, 91191 Gif sur Yvette Cedex, France

<sup>7</sup> IPNL, IN2P3-CNRS/Université Claude Bernard, 69622 Villeurbanne Cedex, France

Received:date / Revised version:date

**Abstract.** High-spin states in the  $^{142}\text{Ce}$  and  $^{140}\text{Ba}$  nuclei have been populated in the  $^{12}\text{C} + ^{238}\text{U}$  and  $^{18}\text{O} + ^{208}\text{Pb}$  fusion-fission reactions at 90 MeV and 85 MeV bombarding energy, respectively. The emitted  $\gamma$ -radiation was detected using the Euroball III and IV arrays. The high-spin yrast and near-to-yrast structures of  $^{142}\text{Ce}$  have been considerably extended. The level scheme of  $^{140}\text{Ba}$  has been extended by six new levels. The newly observed structures in these  $N = 84$  isotones are discussed by analogy with the neighbouring nuclei.

**PACS.** 21.10.Re-k Properties of nuclei; nuclear energy levels – 21.10.Re Collective levels – 23.20.Lv Gamma transitions and level energies – 27.60. +j  $90 \leq A \leq 149$

## 1 Introduction

The yrast structures of the  $N = 84$  isotones from  $^{134}_{50}\text{Sn}$  to  $^{148}_{64}\text{Gd}$  are the result of the competition between the excitations from the two neutrons outside the neutron shell closure and the proton excitations, which are expected to change progressively as the proton Fermi level moves within the  $\pi g_{7/2}$  and  $\pi d_{5/2}$  orbits.

The high-spin levels of the heaviest isotones,  $^{148}_{64}\text{Gd}$ ,  $^{146}_{62}\text{Sm}$ , and  $^{144}_{60}\text{Nd}$ , have been well studied using fusion-evaporation reactions [1–4], while spontaneous fission has been used to populate the yrast states in the lightest isotones,  $^{140}_{56}\text{Ba}$ ,  $^{138}_{54}\text{Xe}$ ,  $^{136}_{52}\text{Te}$ , and  $^{134}_{50}\text{Sn}$  [5, 6]. On the other hand the knowledge of  $^{142}_{58}\text{Ce}$  is very fragmentary. Its first yrast states, up to the  $6^+$  state at 1742 keV, have been mainly identified through inelastic neutron scattering [7, 8] and three new yrast levels have been recently added using deep-inelastic reactions [9].

We report here on new high-spin excited states in  $^{142}\text{Ce}$  and  $^{140}\text{Ba}$ , populated in fission induced by heavy ions.

Their level schemes have been extended up to 6.9 MeV and 5.4 MeV excitation energy, respectively. The newly observed structures are discussed by analogy with the neighbouring nuclei, the isotopes with  $N = 82$  give the properties of the yrast states coming only from the proton excitations, while the excited states of  $^{134}_{50}\text{Sn}$  and  $^{148}_{64}\text{Gd}$  can be traced back to the neutron excitations.

## 2 Experimental methods

The high-spin states in  $^{142}\text{Ce}$  and  $^{140}\text{Ba}$  have been populated using the two fusion-fission reactions,  $^{12}\text{C} + ^{238}\text{U}$  and  $^{18}\text{O} + ^{208}\text{Pb}$  at 90 MeV and 85 MeV incident energy, respectively. For the first experiment, the beam was provided by the Legnaro XTU tandem accelerator, and for the second one by the Vivitron accelerator at IReS (Strasbourg). The targets of 47 mg/cm<sup>2</sup>  $^{238}\text{U}$  and 100 mg/cm<sup>2</sup>  $^{208}\text{Pb}$  were thick enough to stop the recoiling nuclei. The  $\gamma$ -rays were detected with the Euroball III and IV arrays [10], respectively. The spectrometers contained 15 Cluster germanium detectors placed in the backward hemisphere with respect to the beam, 26 Clover germanium detectors located around 90°, and 30 tapered single-crystal germanium detectors located at forward angles. Each Cluster detector consists of seven closely packed

<sup>a</sup> Present address: IPN, IN2P3-CNRS / Université Paris-Sud, 91406 Orsay, France

<sup>b</sup> Present address: Commissariat à l'Énergie Atomique, CEA/DSM Département de Recherches sur la Fusion Contrôlée, 13108 Saint-Paul lez Durance, France

large-volume Ge crystals [11] and each Clover detector consists of four smaller Ge crystals [12].

The data were recorded in an event-by-event mode with the requirement that a minimum of five (three) unsuppressed Ge detectors fired in prompt coincidence and about  $1.9 \times 10^9$  ( $4 \times 10^9$ ) three- and higher-fold coincidence events were registered in the first (second) experiment. The data from the first experiment were sorted with the EURO14 software [13] and analysed using the Radware package [14]. For the second experiment, the offline analysis included both usual  $\gamma$ - $\gamma$  sorting and multi-gated spectra using the Fantastic software [15] and several three-dimensional "cubes" built and analysed with the Radware package [14]. The placement of the  $\gamma$  ray transitions in the level scheme is based on  $\gamma$ - $\gamma$ - $\gamma$  coincidences and relative  $\gamma$ -ray intensities. In such experiments, the uncertainties on the  $\gamma$ -ray energies are 0.15-0.3 keV for  $E_\gamma < 0.75$  MeV and 0.3-0.5 keV for  $0.75 \text{ MeV} < E_\gamma < 1.5$  MeV, depending on their intensity.

The fact that prompt  $\gamma$ -rays emitted by the complementary fragments are detected in coincidence [16,17] has been used to verify the identification of the new transitions. For  $^{142}\text{Ce}$ , the main complementary fragments are  $^{97-100}\text{Zr}$  and  $^{78}\text{Ge}$  for the first and the second reaction, respectively, while for  $^{140}\text{Ba}$  they are  $^{100-102}\text{Mo}$  and  $^{80}\text{Se}$ . The statistics of our  $^{142}\text{Ce}$  and  $^{140}\text{Ba}$  data was too low to perform  $\gamma$ -ray angular correlation analysis of the new transitions observed in this work, so the spin assignments of the new high-spin states are based (i) on the assumption that in the yrast decays spin values increase with excitation energy and (ii) on the analogy with the level structures of the well-known neighbouring nuclei.

### 3 Experimental results

#### 3.1 Study of $^{142}\text{Ce}$

Previous information regarding the  $^{142}\text{Ce}$  low-lying excited states comes from Coulomb excitation,  $\beta$ -decay,  $(t, p)$  reactions, and electron scattering [18]. Through inelastic neutron scattering [7,8], the yrast levels have been firmly established up to the  $6^+$  state at 1742 keV. They have been recently extended with the  $8^+$ ,  $9^{(-)}$  and  $11^{(-)}$  levels using deep-inelastic reactions [9].

The  $^{142}\text{Ce}$  yrast sequence, 641.0-577.6-523.1 keV, as well as the 881.4-369.6-838.7 keV transitions proposed in ref. [9], have been confirmed by our data analysis (see the double-gated spectrum set on 881.4 and 369.6 keV transitions in fig. 1). Using all the mutual  $\gamma$ - $\gamma$ - $\gamma$  coincidences newly observed, we have extended the level scheme up to 6.9 MeV excitation energy, as shown in fig. 2.

The part of the level scheme built on the 2209 keV level (displayed in the right part of fig. 2) has been observed for the first time. As an example, the spectrum gated on the new 248.4 keV and 370.0 keV lines displayed in fig. 1 shows the existence of the new 678.7(522.9+155.8)-370.0-450.3 keV sequence, which populates the  $6^+$  yrast level through the 1114.4 keV transition and the cascade of the 647.0, and 467.3 keV transitions.

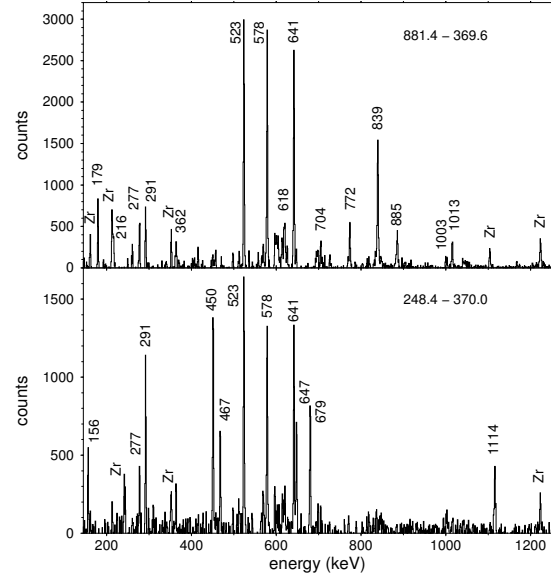


**Fig. 1.** Double-gated spectra set on two transitions of  $^{142}\text{Ce}$ , built from the data obtained in the fusion reaction  $^{12}\text{C}+^{238}\text{U}$  at 90 MeV beam energy. Transitions emitted by the Zr complementary fragments are marked.

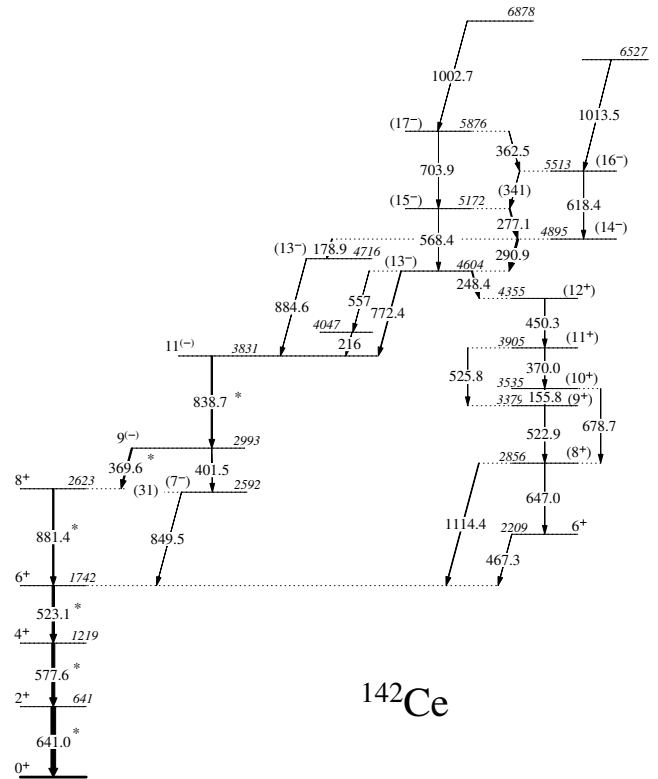


**Fig. 2.** Level scheme of  $^{142}_{58}\text{Ce}_{84}$  obtained as fission fragment in the fusion reactions  $^{12}\text{C}+^{238}\text{U}$  at 90 MeV beam energy and  $^{18}\text{O}+^{208}\text{Pb}$  at 85 MeV beam energy. The transitions marked with a star were already known [9].

A 2.22 MeV excited state had been observed in inelastic electron scattering, with a form factor well described when assuming  $J^\pi = 6^+$  [19]. Moreover a  $J^\pi = 6^+$  level at 2210 keV had been proposed in ref. [7] from inelastic neutron scattering, but has not been firmly confirmed in a later experiment [8]. It can be assumed that the 2209 keV level measured in our work is the same as these  $6^+$  states. Nevertheless contrary to the results quoted in ref. [7], its direct decay to the 1219 keV level is not observed in our experiment: The branching ratio of the 991 keV transition would be less than 5%, as compared to 20% given in ref. [7].

One can remark that the band built on the 2209 keV state is quite similar to the ones built on the  $6^+$  level at 2218 keV in  $^{144}\text{Nd}$  and on the  $6^+$  level at 2223 keV in  $^{146}\text{Sm}$  [3], the level energies as well as the links to the yrast states are almost the same.

Concerning the low-lying octupole states in  $^{142}\text{Ce}$ , the previously known  $3^-$  and  $(5^-)$  states [18] were not populated enough to be observed in our experiments. Following the systematics of ref. [9], the  $(7^-)$  state in  $^{142}\text{Ce}$  is expected to be close in energy to the  $8^+$  yrast state. From our data analysis a new level at 2592 keV has been assigned as the  $(7^-)$  state decaying to the  $6^+$  yrast level through the 849.5 keV transition. The 467 keV transition which may link the  $(7^-)$  and  $(5^-)$  states has not been observed, as expected by comparison with the decay of the  $9^-$  state (the E2 transition is less favored than the E1 one).

Above 4.5 MeV excitation energy, the level scheme of  $^{142}\text{Ce}$  (see fig. 2) comprises three parallel structures which can be organized as a  $\Delta I = 1$  sequence with  $\Delta I = 2$  crossover transitions. Such a behaviour displaying a strong  $\Delta I = 1$  sequence has been also observed in the three heavier isotones,  $^{144}\text{Nd}$ ,  $^{146}\text{Sm}$ , and  $^{148}\text{Gd}$ , in the same energy range. From the results of  $\gamma$  angular distributions and electron conversion coefficients [2, 20, 21], a negative parity has been *firmly* assigned to all the corresponding states in  $^{148}\text{Gd}$  and most of such states in  $^{146}\text{Sm}$  and  $^{144}\text{Nd}$ . We also adopt a negative parity for this group of states in  $^{142}\text{Ce}$ . Then the assignment of  $I^\pi = (13^-)$  to the state at 4604 keV is determined because of its decay towards a  $(12^+)$  state and a  $11(-)$  state.

### 3.2 Results on $^{140}\text{Ba}$

The medium-spin states of  $^{140}\text{Ba}$  has been already studied and discussed in ref. [5]. Thanks to the fusion-fission reactions used in the present work, a few states with higher spin values have been observed in this nucleus, as shown in fig. 3. Whereas the known  $3^-$  level [5] has not been populated in our two experiments, a new 491.5 keV line deexciting the  $(5^-)$  level has been measured. Moreover a new level at 2800 keV decaying to the  $6^+$  yrast state has been identified. A spin value of  $(8^+)$  is proposed for this level. Because of experimental limitations (this isotope is located at the edge of the production zone), we could not observe the structure built on this  $(8^+)$  level.

The high-spin part of the  $^{140}\text{Ba}$  level scheme has been extended by five new levels above 3770 keV excitation

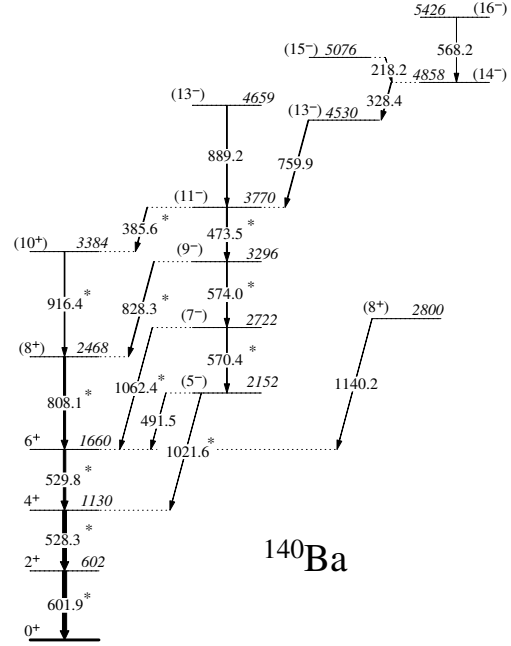


**Fig. 3.** Level scheme of  $^{140}\text{Ba}_{84}$  obtained as fission fragment in the fusion reactions  $^{12}\text{C} + ^{238}\text{U}$  at 90 MeV beam energy and  $^{18}\text{O} + ^{208}\text{Pb}$  at 85 MeV beam energy. The transitions marked with a star were already known [5].

energy. The sequence of states at 4530, 4659, 4858, 5076, and 5426 keV is similar to the group of negative-parity states newly observed in  $^{142}\text{Ce}$ , their excitation energies as well as their decay properties are the same.

## 4 Discussion

The main part of the discussion is devoted to  $^{142}\text{Ce}$  in which many new high-spin structures have been identified. According to the shell model, the configuration of its ground state involves a rather small number of valence nucleons, only 8 protons and 2 neutrons outside the doubly-magic  $^{132}\text{Sn}_{82}$  core. Moreover, it is well known that  $^{146}\text{Gd}_{82}$  behaves as a doubly-closed nucleus, indicating that for  $N = 82$  there is a sub-shell closure at  $Z = 64$ , between two groups of orbits belonging to the major shell, i.e. the  $\pi g_{7/2}$  and  $\pi d_{5/2}$  orbits in the one hand, the  $\pi h_{11/2}$ ,  $\pi d_{3/2}$ , and  $\pi s_{1/2}$  orbits in the other hand. Hence it is expected that the *yrast* levels of all the  $N = 84$  isotones with  $Z = 50 - 64$  would display smooth changes, which can be understood in a qualitative way by considering the occupation of a few number of high- $j$  orbitals by the valence nucleons. Furthermore negative-parity states from octupole correlations are known to be located at low energy in this mass region.

The energies of the first fully-aligned states coming from one neutron-pair breaking in the  $N = 84$  isotones with  $50 \leq Z \leq 64$  [1–6] are drawn in the right part of fig. 4. The main configuration of the  $6^+_1$  level is  $(\nu f_{7/2})^2$

and the one of the  $8_1^+$  level,  $(\nu f_{7/2})^1(\nu h_{9/2})^1$ , these neutron excitations being likely mixed with proton excitations (discussed in the following paragraph) for  $Z = 52 - 62$ . Moreover, the coupling of the one-octupole phonon to the

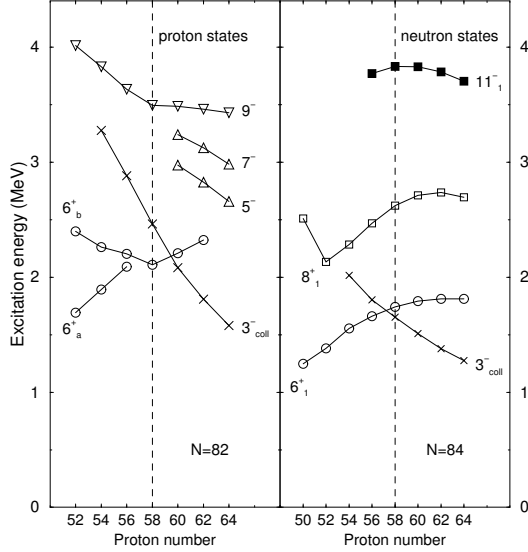


**Fig. 4.** Elementary excitations expected at low excitation energy in the  $N = 84$  isotones as a function of the proton number. The octupole mode and the neutron excitations, displayed in the right part, are those measured in the  $N = 84$  isotones. The proton excitations, drawn in the left part, come from the  $N = 82$  isotones. The detailed configurations are given in the text.

$8_1^+$  state gives the yrast  $11^-$  state with an almost constant excitation energy (see the right part of fig. 4), as for increasing  $Z$ , the  $3^-$  state displays a decrease in energy whereas  $8_1^+$  state increases in energy. The 3831 keV state of  $^{142}\text{Ce}$  fits well in this evolution.

Concerning the *proton* excitations which can be foreseen in the  $N = 84$  isotones, they can be easily deduced from the levels observed in the isotopes having  $N = 82$ . The energies of the first fully-aligned states coming from one proton-pair breaking in the  $N = 82$  isotones with  $52 \leq Z \leq 64$  [22–28] are drawn in the left part of fig. 4. The first  $6^+$  state of  $^{134}\text{Te}$ ,  $^{136}\text{Xe}$ , and  $^{138}\text{Ba}$  (noted  $6_a^+$  in the figure) comes from  $\pi g_{7/2}$ , the first orbit located above  $Z = 50$ . On the other hand, the configuration of the  $6_b^+$  state which has been identified from  $Z = 52$  to  $Z = 62$  involves both the  $\pi g_{7/2}$  and  $\pi d_{5/2}$  orbits. Since these two proton orbits are completely filled for  $Z = 64$ , no  $6^+$  state is observed at low energy in  $^{146}\text{Gd}$ . It is noteworthy that the  $6_b^+$  energy, which mainly depends on the location of the Fermi level within the two proton orbits, is minimal at  $Z = 58$  as expected.

A proton configuration can be assigned to the second  $6^+$  state at 2209 keV in  $^{142}\text{Ce}$  and we interpret the structure built on this state (see fig. 2) as  $(\pi g_{7/2})^1(\pi d_{5/2})^1 \otimes (\nu f_{7/2})^2$ , the fully-aligned state having  $I^\pi = 12^+$ . The

same configuration can be assigned to the similar structures observed in  $^{144}\text{Nd}$  and in  $^{146}\text{Sm}$  [3] in the same energy range, as said above. No configuration assignment had been given in that publication which was mainly dealing with the investigation of double-octupole excitations.

For  $50 \leq Z \leq 82$ , the maximum spin value with negative parity which can be obtained from the breaking of one proton pair,  $I^\pi = 9^-$ , involves the two high- $j$  orbits,  $\pi g_{7/2}$  and  $\pi h_{11/2}$ . This state, identified in all the  $N = 82$  isotones with  $Z = 52 - 64$ , is drawn in the left part of fig. 4. It is worth pointing out that for  $Z \geq 60$ , the  $\pi d_{5/2}$  orbit is located closer to the proton Fermi level than the  $\pi g_{7/2}$  one. Then in  $^{142}\text{Nd}$ ,  $^{144}\text{Sm}$ , and  $^{146}\text{Gd}$ , the  $(\pi d_{5/2})^{-1}(\pi h_{11/2})^1$  proton-pair breaking gives rise to states with lower spin values at lower excitation energies than that of the  $9^-$  state from  $(\pi g_{7/2})^{-1}(\pi h_{11/2})^1$ . The  $I^\pi = 5^-$  and  $7^-$  states known in  $^{142}\text{Nd}$ ,  $^{144}\text{Sm}$ , and  $^{146}\text{Gd}$  are drawn in the left part of fig. 4.

In the  $N = 84$  isotones, the coupling of these negative-parity proton configurations to the positive-parity neutron ones, mentioned above, would result in excited states with spin values up to  $17^-$ . Moreover as such coupled configurations contain both particles and holes, strong M1 transitions are expected between the members of the multiplets. In  $^{148}\text{Gd}$  and  $^{144}\text{Nd}$ , the negative-parity structures displaying the strong  $\Delta I = 1$  sequence identified above 4 MeV excitation energy have been interpreted in terms of such couplings [2, 4]. Then the configurations,  $(\pi g_{7/2})^{-1}(\pi h_{11/2})^1 \otimes (\nu f_{7/2})^2$  or  $(\nu f_{7/2})^1(\nu h_{9/2})^1$ , can be also assigned to the states of  $^{142}\text{Ce}$  identified above 4.5 MeV excitation energy (see fig. 2). Unlike the heavy isotones, the negative-parity structure of  $^{142}\text{Ce}$  does not extend below spin  $13^-$ . This could be correlated to the change of the *yrast* proton states when the proton Fermi level moves within the major shell. As said above, whereas the  $(\pi g_{7/2})^{-1}(\pi h_{11/2})^1$  configuration is yrast for  $Z = 52 - 58$ , the configuration involving the  $\pi d_{5/2}$  orbit gives several states having lower spin values and lower energy, as soon as  $Z \geq 60$ .

As regards to  $^{140}\text{Ba}$ , its medium-spin structure has been already discussed in connection with those observed in the heavier Ba isotopes displaying octupole correlations [5], particularly its negative-parity states with  $E < 4$  MeV which are quite regularly spaced in energy and strongly connected to the positive-parity yrast states. Nevertheless, the new levels we have newly identified above the  $(13^-)$  state at 4530 keV (see fig. 3) bear strong resemblance to those in  $^{142}\text{Ce}$  and can be also interpreted in terms of single-particle excitations,  $(\pi g_{7/2})^{-1}(\pi h_{11/2})^1 \otimes (\nu f_{7/2})^2$  or  $(\nu f_{7/2})^1(\nu h_{9/2})^1$ .

## 5 Summary

In the present work, the high-spin level scheme of  $^{142}\text{Ce}$  has been extended up to 6.9 MeV excitation energy, it displays several band structures in parallel. Moreover in  $^{140}\text{Ba}$ , we have identified new high-spin levels above 4 MeV excitation energy. The spin and parity values of all

these new states have been assigned from the analogy (excitation energy and main decay mode) with the neighbouring nuclei. All the structures of  $^{142}\text{Ce}$  have been discussed in terms of neutron excitations dealing with the two first neutron subshells located above the  $N = 82$  magic number, i.e.  $\nu f_{7/2}$  and  $\nu h_{9/2}$ . Moreover the two positive-parity high- $j$  proton subshells,  $\pi g_{7/2}$  and  $\pi d_{5/2}$ , are involved in the newly observed structure based on the  $6^+$  state at 2.2 MeV excitation energy. Above 4.5 MeV excitation energy, both the  $^{142}\text{Ce}$  and  $^{140}\text{Ba}$  level schemes are governed by negative-parity states displaying strong  $\Delta I = 1$  sequences, they involve the highest- $j$  proton orbit in the major shell,  $\pi h_{11/2}$ . This indicates that single-proton excitations play a major role in the high-spin yrast states of these  $N = 84$  isotones.

The Euroball project was a collaboration between France, the United Kingdom, Germany, Italy, Denmark and Sweden. This work has been supported in part by the collaboration agreement BAS-CNRS under contract No. 16946. The Euroball III experiment has been performed under U.E. contract (ERB FHGECT 980 110) at Legnaro. The Euroball IV experiment has been supported in part by the EU under contract HPRI-CT-1999-00078 (EUROVIV). We thank the crews of the tandem of Legnaro and of the Vivitron. We are very indebted to M.-A. Saetle for preparing the Pb targets, P. Bednarczyk, J. Devin, J.-M. Gallone, P. Médina, and D. Vintache for their help during the Euroball IV experiment.

## References

1. S. Lunardi et al., Phys. Rev. Lett. **53**, 1531 (1984)
2. M. Piiparinen et al., Z. Phys. A **337**, 387 (1990)
3. L. Bargioni et al., Phys. Rev. C **51**, R1057 (1995)
4. J.K. Jewell et al., Phys. Rev. C **52**, 1295 (1995)
5. W. Urban et al., Nucl. Phys. A **613**, 107 (1997)
6. A. Korgul et al., Eur. Phys. J. A **7**, 167 (2000)
7. M.M. Alhamidi et al., Sov. J. Nucl. Phys. **55**, 496 (1992)
8. J.R. Vanhoy et al., Phys. Rev. C **52**, 2387 (1995)
9. Z. Liu et al., Eur. Phys. J. A **13**, 277 (2002)
10. J. Simpson, Z. Phys. A **358**, 139 (1997) and F.A. Beck, Prog. Part. Nucl. Phys. **28**, 443 (1992)
11. J. Eberth et al., Nucl. Instrum. Methods A **369**, 135 (1996)
12. G. Duchêne et al., Nucl. Instrum. Methods A **432**, 90 (1999)
13. Ch. Theisen, Euro 14 sorting package, unpublished
14. D. Radford, Nucl. Instrum. Methods A **361**, 297; 306 (1995)
15. I. Deloncle, M.-G. Porquet, M. Dziri-Marcé, Nucl. Instrum. Methods A **357**, 150 (1995)
16. M.A.C. Hotchkis et al., Nucl. Phys. A **530**, 111 (1991)
17. M.G. Porquet et al., Acta Phys. Polon. B **27**, 179 (1996)
18. J.K. Tuli, Nucl. Data Sheets **89**, 641 (2000)
19. W. Kim et al., Phys. Rev. C **44**, 2400 (1991)
20. L.K. Peker and J. K. Tuli, Nucl. Data Sheets **82**, 187 (1997)
21. A.A. Sonzogni, Nucl. Data Sheets **93**, 599 (2001)
22. S. K. Saha et al., Phys. Rev. C **65**, 017302 (2001)
23. P. J. Daly et al., Phys. Rev. C **59**, 3066 (1999)
24. A.A. Sonzogni, Nucl. Data Sheets **98**, 515 (2003)
25. W. Enghardt et al., Z. Phys. A **316**, 245 (1984)
26. R. Wirowski et al., Z. Phys. A **329**, 509 (1988)
27. E. Ott et al., Z. Phys. A **348**, 57 (1994)
28. P. Kleinheinz et al., Z. Phys. A **290**, 279 (1979)